Volcanic Ash Cloud Properties: Comparison Between MODIS Satellite Retrievals and FALL3D Transport Model

Stefano Corradini, Luca Merucci, and Arnau Folch

***Abstract*—The moderate Resolution Imaging Spectroradiometer (MODIS) is a multispectral satellite instrument operating from the visible to thermal infrared spectral range. FALL3D is a 3-D time-dependent Eulerian model for the transport and deposition of volcanic particles. In this letter, quantitative comparison between the volcanic cloud ash mass and optical depth retrieved by MODIS and modeled by FALL3D has been performed. Three MODIS images collected on October 28, 29, and 30 on Mt. Etna volcano during the 2002 eruption have been considered as test cases. The results show a general good agreement between the retrieved and the modeled volcanic clouds in the first 300 km from the vents. Even if the modeled volcanic cloud area is systematically wider than the retrieved area, the ash total mass is comparable and varies between 35 and 60 kt and between 20 and 42 kt for FALL3D and MODIS, respectively. The mean aerosol optical depth (AOD) values are in good agreement and approximately equal to 0.8. When the whole volcanic clouds are considered the ash areas, then the total ash masses, computed by FALL3D model, are significantly greater than the same parameters retrieved from the MODIS data, while the mean AOD values remain in very good agreement and equal to about 0.6. The volcanic cloud direction in its distal part is not coincident for the October 29 and 30, 2002 images due to the difference between the real and the modeled local wind fields. Finally, the MODIS maps show regions of high mass and AOD due to volcanic puffs not modeled by FALL3D.**

***Index Terms*—FALL3D transport model, Moderate Resolution Imaging Spectroradiometer (MODIS) measurements, remote sensing of volcanoes, volcanic ash retrievals, volcanic hazard and risk.**

I. Introduction

DUE TO the large emission of gas and solid particles into the atmosphere, volcanic eruptions are one of the most important source of natural pollution. The most abundant gases released are water vapor (H_2O), carbon dioxide (CO_2), sulphur dioxide (SO_2), and hydrochloric acid (HCl). In addition, volcanoes emit particles of different sizes. The term volcanic ash refers to particles with sizes ranging from millimeter to less than 1 μm. The size, density, and shape of a particle determine its residence time in the atmosphere. Typically, particles with radius larger than 100 μm have short residence times (from minutes to hours), while particles smaller than 10 μm and gaseous aerosols can remain airborne from days to weeks and travel hundreds to thousands of kilometers downwind as a volcanic ash cloud.

The assessment of properties, movement, and extent of volcanic ash clouds is an important scientific, economic, and public safety issue because of its effects on the environment [1], climate [2], public health [3], and, in particular, aerial navigation [4]. All of the cited requirements make it essential to have a greater effort to realize robust and affordable ash cloud detection and trajectory forecasting, combining remote sensing and modeling.

Because of the sporadic nature and the large spatial extent of ash dispersal during volcanic eruptions, satellite remote sensing is the most suitable technique to detect ash clouds and to retrieve relevant physical properties. A procedure based on the difference between the brightness temperature of two channels centered around 11 and 12 μm and on radiative transfer models is commonly used for both detection and retrieval purposes [5], [6]. Such technique has been applied to different polar and geostationary satellite systems such as the Advanced Very High Resolution Radiometer [6], [7], the Moderate Resolution Imaging Spectroradiometer (MODIS) [8], the Geostationary Operational Environmental Satellite (GOES) [9], and the Spin Enhanced Visible and Infrared Imager measurements [10]. The procedure allows to retrieve ash effective radius, aerosol optical depth (AOD), cloud mass, and cloud extent. In parallel to remote sensing, ash dispersal models are routinely used by Volcanic Ash Advisory Centers to foresee short-term (next 24–48 h) dispersion of ash clouds and by Volcano Observatories and others to predict the amount of expected fallout. Compared to remote sensing, models can deal with the whole spectrum of particle sizes but, in contrast, require inputs that are poorly constrained during an eruption. In this scenario, relevant input values must be assumed or inferred from some other observable. For example, the eruption rate can be estimated indirectly from the plume height using empirical fits [11, p. 574] or the buoyant plume theory (BPT) [12], but uncertainties remain large.

Remote sensing retrievals are necessary to validate transport models and, ideally, should also be used to improve model initialization by means of data assimilation. Conversely, simulations of well-studied past events can be used to test the accuracy of the retrieval techniques. Surprisingly, comparative studies between models and satellite retrievals are very scarce

Manuscript received March 3, 2010; revised May 17, 2010; accepted July 12, 2010. Date of publication September 9, 2010; date of current version February 25, 2011. This work was supported by the SAVAA project founded by the European Space Agency.

S. Corradini and L. Merucci are with the Istituto Nazionale di Geofisica e Vulcanologia (INGV), 00143 Rome, Italy (e-mail: stefano.corradini@ingv.it; luca.merucci@ingv.it).

A. Folch is with the Barcelona Supercomputing Center, 08034 Barcelona, Spain (e-mail: arnau.folch@bsc.es).

Digital Object Identifier 10.1109/LGRS.2010.2064156

yet [13]. In this letter, we perform a quantitative comparison between the ash mass and AOD at 0.55 μm from MODIS satellite measurements and FALL3D dispersal model [14], [15]. The volcanic cloud overlap is also computed. As test cases, we focus on the Mt. Etna October 28–30, 2002 eruptive events.

II. Test Case Description—Mt. Etna 2002 Eruption

Mt. Etna (37.73° N, 15.00° E), a massive stratovolcano (3330 m a.s.l.) located in the eastern part of Sicily (Italy), is one of the major degassing volcanoes in the world. Etna's general quiescent state is periodically interrupted by eruptive crises during which significant emissions of gases and ash occur. Ash fallout periodically reaches the surrounding areas affecting the local population and disrupting the nearby Catania, Sigonella, and Reggio Calabria airports.

The Mt. Etna 2002 eruption began on the evening of October 26 with a swarm of earthquakes recorded by the Italian National Institute of Geophysics and Volcanology. The seismic swarm preceded and accompanied the explosive activity in the northeast and south volcano flanks and strombolian activity in the summital area. The explosive activity increased during the following days reaching a paroxysm during October 28–31, with a fairly sustained eruptive column that rose up to 7 km a.s.l. [16]. Ash fallout caused many problems to the surrounding population and infrastructures, including the closure of the Catania Fontanarossa (October 27) and the Reggio Calabria (October 31) airports. Prevailing winds directed the ash cloud toward the African coast, causing a light fallout in Libya (≈600 km from Mt. Etna) during the subsequent days [17].

In this letter, the October 28, 29, and 30, 2002 images collected at 12:15, 09:45, and 12:05 UTC, respectively, by MODIS-Aqua (October 28 and 30) and MODIS-Terra (October 29), have been considered as test cases.

III. Ash Retrieval From TIR MODIS Images

MODIS is a satellite multispectral instrument with 36 spectral bands in the wavelength range from the visible (VIS) to thermal infrared (TIR) (http://modis.gsfc.nasa.gov/). The ash detection in the TIR spectral range is carried out by using the brightness temperature difference (BTD) procedure [5] applied to the channels centered around 11 and 12 μm (MODIS channels 31 and 32, 1 km ground spatial resolution). The ash retrievals (effective radius (r_e) and AOD at 0.55 μm) are obtained from the top-of-atmosphere (TOA) simulated "inverted arches" curves BTD versus brightness temperature at 11 μm by varying AOD and r_e [6]. To reduce the water vapor masking effects on BTD, a water vapor correction procedure has also been applied [8]. The ash mass is computed pixel-by-pixel exploiting the simplified formula suggested by Wen and Rose [6]

$$M(n,m) = \frac{4}{3}\frac{S\rho r_e^{(n,m)} AOD^{(n,m)}}{Q_{ext}\left(r_e^{(n,m)}\right)} \tag{1}$$

where S is the pixel surface, ρ is the particle density, $r_e^{(n,m)}$ is the effective radius of pixel (n,m), $AOD^{(n,m)}$ is the aerosol optical depth of pixel (n,m), and $Q_{ext}(r_e^{(n,m)})$ is the extinction efficiency factor at effective radius $r_e^{(n,m)}$.

TABLE I
FALL3D Input Values for Column Height (in Meters Above the Vent) and Resulting MER According to the BPT

Event	Time Interval [h after 00UTC]	Column Height [m a.v.]	Averaged MER [kg/s]
28 Oct 2002	00:00-06:00	3750	1.6×10^5
	06:00-12:00	4000	2.2×10^5
	12:00-18:00	4250	3×10^5
	18:00-24:00	4000	3×10^5
29 Oct 2002	00:00-06:00	3500	2×10^5
	06:00-12:00	3000	1.5×10^5
	12:00-18:00	3250	2×10^5
	18:00-24:00	3500	2×10^5
30 Oct 2002	00:00-06:00	3750	2.1×10^5
	06:00-12:00	4000	2.3×10^5

The TOA simulations have been performed by using MODTRAN radiative transfer model by using different input parameters as the atmospheric profiles [pressure, temperature, and humidity (PTH)], the surface temperature and emissivity, the volcanic cloud geometry (altitude and thickness), and the ash optical properties. For each MODIS image, the PTH profiles derive from the Weather Research and Forecasting (WRF) model [18], a fully compressible nonhydrostatic mesoscale meteorological model. The volcanic cloud altitudes are derived from Andronico *et al.* [16] that show analyses of eruption images and videos. The sea surface temperature is computed by inverting the radiative transfer equation in the TIR spectral range [10] using the MODIS channels 31 and 32, and considering as emissivity the sea surface values extracted by the ASTER spectral emissivity library database (http://speclib.jpl.nasa.gov/), considering the MODIS response functions. Because the volcanic cloud is not transparent at these wavelengths, the underneath sea surface temperature has been assumed as the mean temperature of two wide regions selected just outside the cloud area [8], [10]. The volcanic dust optical properties [19] with log-normal size distribution and particle density equal to 2500 kg/m^3 have been also considered [20].

The ash retrieval errors have been set to 40% and 30% for total ash mass and mean AOD, respectively, and derived from a sensitivity study carried out by [8] considering the uncertainties of the different input MODTRAN parameters. The sensitivity limit on particle effective radius, in the considered TIR spectral range, varies between 0.8 and 10 μm, while the minimum AOD retrievable is 0.1.

IV. FALL3D Dispersion Model

FALL3D [14], [15] is a Eulerian model for transport and deposition of tephra. The model solves an advection-diffusion-sedimentation equation for each particle class, characterized by its diameter, density, and shape factor. The main volcanological inputs are the mass eruption rate (MER) and the total grain size distribution. The outputs of the model are the time-dependent load at surface (i.e., accumulation rate and deposit thickness) and atmospheric ash concentration (i.e., mass per unit volume for each particle class). The AOD is computed at each point

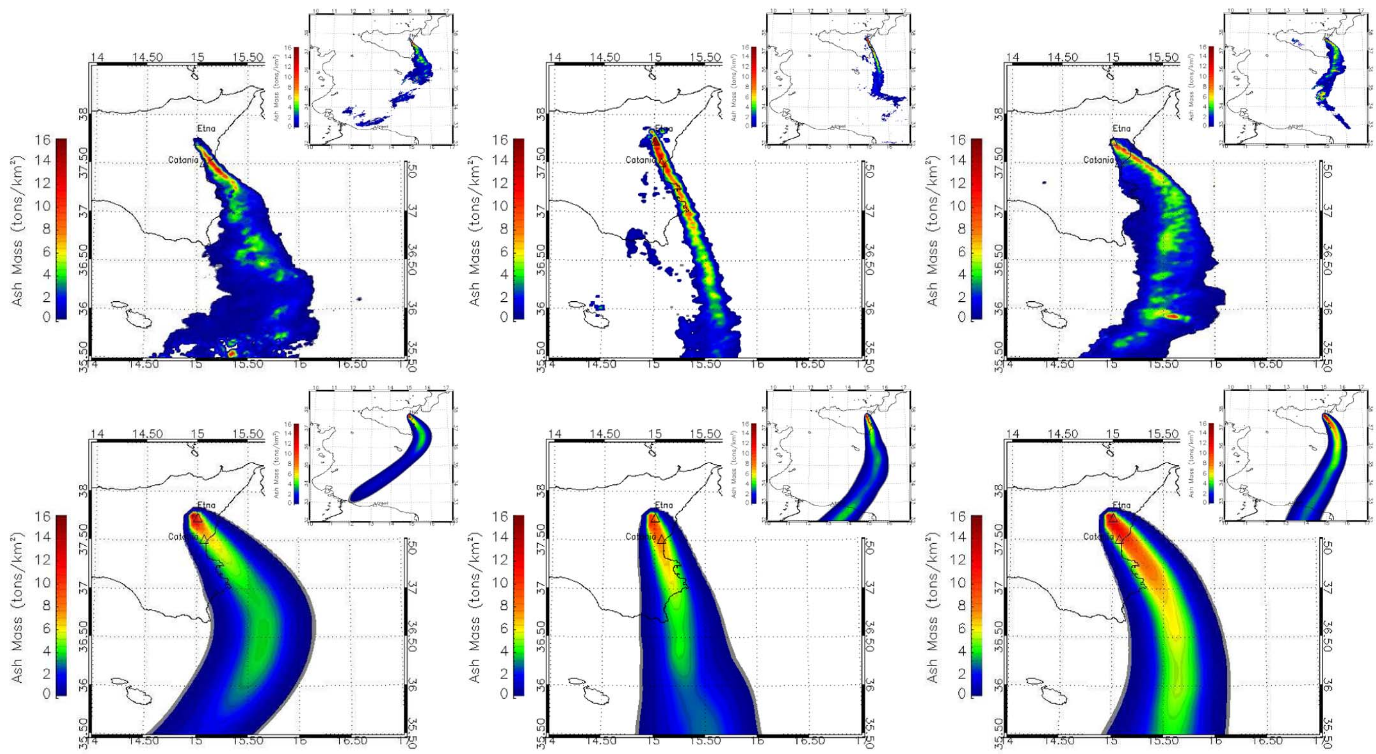

Fig. 1. Total ash mass maps. (Left to right) October 28, 29, and 30, 2002. (Upper plates) MODIS retrieved maps. (Lower plates) FALL3D-modeled maps.

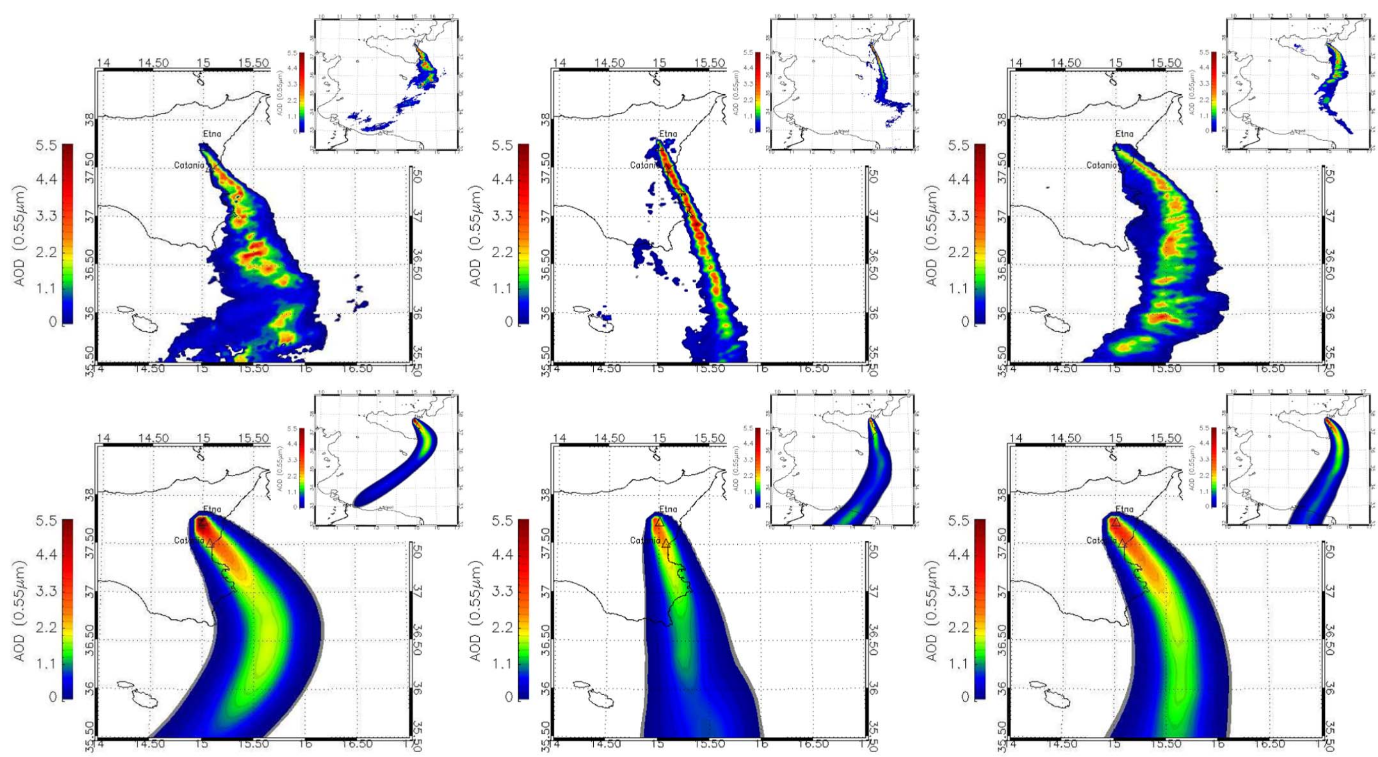

Fig. 2. AOD at 0.55 μm maps. (Left to right) October 28, 29, and 30, 2002. (Upper plates) MODIS retrieved maps. (Lower plates) FALL3D-modeled maps.

from the column mass using (1) and taking into account all particle classes with diameter ≤ 10 μm.

In order to obtain the meteorological variables, we coupled FALL3D with the WRF model. The WRF model was configured to integrate the primitive equations using the advanced research WRF dynamics solver in a two-nest domain (15 and 5 km resolution, respectively) with 64 vertical layers and top model pressure of 50 hPa. Initial and 6-hourly boundary conditions for WRF were obtained from the National Centers for Environmental Prediction-2 reanalysis.

TABLE II
TOTAL ASH MASSES (T_M), MEAN AOD AT 0.55 μm AND, PERCENTAGE OF CLOUD OVERLAP FOR THE MODIS AND FALL3D RETRIEVALS. ON EACH ERUPTION DATE, THE FIRST ROW INDICATES THE VALUES OBTAINED CONSIDERING THE WHOLE IMAGES, AND THE SECOND ROW INDICATES THE VALUES OBTAINED CONSIDERING ONLY THE FIRST 300 km FROM THE VENTS (SEE ZOOMED IMAGES)

Date	MODIS			FALL3D			% cloud overlap	% cloud overlap
	Area [km^2]	T_M [kt]	$\overline{AOD}$	Area [km^2]	T_M [kt]	$\overline{AOD}$	AOD $\geq$ 0.1	AOD $\geq$ 1
28 Oct 2002	26700	63.0 $\pm$ 25.2	0.62 $\pm$ 0.19	43700	90.0	0.62	55	66
	15600	41.9 $\pm$ 16.8	0.80 $\pm$ 0.24	19300	61.0	0.97	82	70
29 Oct 2002	13700	30.3 $\pm$ 12.1	0.57 $\pm$ 0.17	61400	106.9	0.53	74	23
	5300	19.4 $\pm$ 7.8	0.91 $\pm$ 0.27	15100	33.8	0.67	95	23
30 Oct 2002	24300	59.5 $\pm$ 23.8	0.59 $\pm$ 0.18	62900	125.8	0.61	82	62
	13100	36.9 $\pm$ 14.8	0.78 $\pm$ 0.23	16900	51.8	0.93	95	64

A. Model Setup

We used FALL3D to simulate Mt. Etna ash clouds from October 28, 2002 at 00 UTC to October 20, 2002 at 12 UTC. The spatial resolution was set to 1.5 km, a value similar to the MODIS TIR bands ground resolution at nadir. The model was configured with the Ganser terminal velocity model and the ##RAMS model parameterization for horizontal diffusion [15] with Cs $= 0.15$ and Prandtl number $\mathrm{Pr} = 1$. In the simulations, we assumed a particle grain size distribution with ten classes ranging in diameter from 1 mm (0Φ) to 1 μm (9Φ) and peaked at 125 μm (3Φ). For simplicity, we assumed constant density (2500 kg/m^3) and sphericity (0.9) for all particle classes. For comparison, Andronico *et al.* [16] found a 3Φ mode and a 1Φ deviation for the samples collected during October 28, 2002 at a distance of 25 km. The fraction of mass with diameter below 10 μm (i.e., entering in the computation of AOD) is of about 4%, consistent with the proportion of very fine ash typically observed in basaltic eruptions [21].

We used time-dependent values for plume heights and MER as reported in Table I. Also, in this case, the plume heights derive from [16] and were determined from the analysis of images and videos. The source terms were estimated by means of the BPT, which allows the computation of the vertical distribution of mass and the MER every hour depending on the column heights and wind field to account for plume bent over. The resulting erupted mass during the simulated period is of 2.8×10^{10} kg (from October 28, 2002 at 00UTC to October 30 at 12UTC). For comparison, Andronico *et al.* [16] give values of about 10^{10} kg for 6 h of fallout during October 28, 2002 and 4.4×10^{10} kg for the October 28–31, 2002 period.

V. RESULTS

The volcanic ash cloud mass per square kilometer and AOD at 0.55 μm evolution modeled by FALL3D are given in the auxiliary material (see "FALL3D_Etna_2002_Tmass_movie.gif" and "FALL3D_Etna_2002_AOD_movie.gif", respectively). The movies show the volcanic cloud movement from October 28 at 00 UTC to October 30 at 12 UTC every 15 min.

In the following discussion, we shall refer to the FALL3D and MODIS ash clouds displayed in Figs. 1 and 2, showing the ash mass per square kilometer and the AOD at 0.55 μm, respectively. Each figure shows, from left to right, the October 28, 29, and 30, 2002 maps retrieved from MODIS (upper Plates) and modeled by FALL3D (lower Plates). The FALL3D ash maps shown are near contemporary to all the MODIS images (i.e., extracted at 12:15, 09:45, and 12:00 UTC for the October 28, 29, and 30, 2002, respectively). Some qualitative results can be noticed at a first sight.

The images show a general good agreement in both the AOD and total mass area series of maps, and this is particularly evident when comparing the ash cloud areas in the first 300 km from the vent (zoomed Plates). The MODIS retrievals emphasize regions of high AOD and total ash mass not captured by FALL3D. These "puffs" are likely caused by short-term oscillations of the eruption intensity. The FALL3D ash cloud areas are always larger and include most of the MODIS ash clouds. This can be justified because the spreading of the volcanic cloud in its distal part causes the ash signal to fade out beyond the detectivity threshold of the retrieval procedure and, moreover, in the same area, many pixels are rejected because it is being affected by meteorological clouds. Finally, both Figs. 1 and 2 show that, for the October 29 and 30, 2002 cases, the directions of the retrieved and modeled clouds in their distal parts (near the African coast) are not coincident. Such a discrepancy can be attributed to different causes such as differences between the real and the WRF-modeled wind fields, incorrect ash release height that can yield to inaccurate modeling of the cloud direction in the presence of strong wind shear (as observed in the 29 and 30 images), or when the ash signal is too weak.

These qualitative observations are quantitatively supported by the results summarized in Table II for the three days of the eruption. The time, area, total mass, and AOD are compared for the MODIS and FALL3D ash clouds, along with the percentage of cloud overlap defined by AOD ≥ 0.1 and AOD ≥ 1. The total volcanic cloud area and ash mass modeled by FALL3D can be more than three times greater than the corresponding MODIS retrievals. Table II also shows the results of areas and total masses computed by considering the zoomed regions only. Here, the differences between the modeled and the retrieved parameters are much less important, except for the October 29 case for which it still remains significant. The October 28 and 30 total ash mass retrieved by MODIS from the whole images (63 and 60 kt) turn out to be comparable with that of the total masses retrieved by [22] (93 and 132 kt) from the nearly contemporaneous Atmospheric Infrared Sounder (AIRS) images, taking into account that a significant part of the ash clouds retrieved from AIRS data is over Africa, in a region that was not framed by the MODIS data. The mean AOD comparison is in very good agreement, always around 0.6 when evaluated on the whole images and higher on the subsets (see Table II). The ash cloud overlaps were computed as the intersection between the MODIS and FALL3D clouds area divided by the MODIS cloud area for AOD ≥ 0.1 and AOD ≥ 1. In the first case (AOD ≥ 0.1), the overlap ranges from 55% to 82% and from 82% to 95% for the subset images (see Table II). The overlap percentages at AOD ≥ 1 show that the maxima of the retrieved and modeled ash clouds do not always overlap. The difference in the overlap percentage obtained by varying the AOD threshold can be interpreted as an indicator of the local accuracy of wind field used by the model. In the 29 October test case, the overlap percentage at AOD ≥ 1 drops to 23% showing that even if the clouds are collocated (AOD ≥ 0.1 ranges from 74% to 95%), the AOD structures of the retrieved and modeled volcanic ash clouds differ.

VI. Conclusions

Volcanic ash cloud parameters retrieved from MODIS satellite data and simulated by FALL3D dispersion model have been quantitatively compared. The mean AOD and total mass show a good agreement not only when they are compared as integrated measures but also when spatially compared as AOD and mass maps of the retrieved and modeled ash clouds. More than the integrated measure comparison, the analysis of ash mass and AOD maps allows the detailed comparison of the retrieved and modeled ash clouds. Three MODIS images collected at 12:15, 9:45, and 12:05 on October 28, 29, and 30, 2002, respectively, on Mt. Etna volcano have been analyzed. The results indicate a good agreement in the first 300 km from the volcano vents. In this area, the total ash mass varies between 20 and 45 kt and between 35 and 60 kt for MODIS and FALL3D, respectively, the mean AOD is about 0.8, and the retrieved and modeled ash clouds are essentially collocated. In contrast, modeled cloud areas and masses are greater than those retrieved from MODIS data when the whole volcanic clouds are considered. However, the mean AOD values still remain in a very good agreement and equal to about 0.6. Reasons to explain such differences in the distal parts include insufficient accuracy in the modeled wind directions and too weak ash signal to be detected by the satellite. The study of the clouds' spatial overlap gives insights on the ash cloud structure and points to the refinements that should be considered in order to improve the matching between retrievals and models.

Acknowledgment

A.F is grateful to the Spanish Ramon y Cajal scientific program. Simulations have been done at the BCS-CNS supercomputing facilities (Barcelona, Spain) using the MareNostrum supercomputer.

References

[1] H. Thordasson and S. Self, "Atmospheric and environmental effects of the 1783-1784 Laki eruption: A review and reassessment," *J. Geophys. Res.*, vol. 108, no. D1, p. 4011, Jan. 2003.

[2] R. G. Grainger and E. J. Highwood, "Changes in stratospheric composition chemistry, radiation and climate caused by volcanic eruptions," in *Volcanic Degassing*, C. Oppenheimer, D. M. Pyle, and M. Barklay, Eds. London, U.K.: Geol. Soc., 2003, pp. 329–347.

[3] C. J. Horwell and P. J. Baxter, "The respiratory health hazards of volcanic ash: A review for volcanic risk mitigation," *Bull. Volcanol.*, vol. 69, no. 1, pp. 1–24, 2006.

[4] T. J. Casadevall, "The 1989/1990 eruption of Redoubt Volcano Alaska: Impacts on aircraft operations," *J. Volcanol. Geotherm. Res.*, vol. 62, no. 30, pp. 301–316, Aug. 1994.

[5] A. J. Prata, "Radiative transfer calculations for volcanic ash clouds," *Geophys. Res. Lett.*, vol. 16, no. D11, pp. 1293–1296, 1989.

[6] S. Wen and W. I. Rose, "Retrieval of sizes and total masses of particles in volcanic clouds using AVHRR bands 4 and 5," *J. Geophys. Res.*, vol. 99, no. D3, pp. 5421–5431, 1994.

[7] A. J. Prata, "Observation of volcanic ash clouds using AVHRR-2 radiances," *Int. J. Remote Sens.*, vol. 10, no. 4/5, pp. 751–761, 1989.

[8] S. Corradini, C. Spinetti, E. Carboni, C. Tirelli, M. F. Buongiorno, S. Pugnaghi, and G. Gangale, "Mt. Etna tropospheric ash retrieval and sensitivity analysis using Moderate Resolution Imaging Spectroradiometer measurements," *J. Atmos. Remote Sens.*, vol. 2, p. 023 550, 2008.

[9] T. Yu, W. I. Rose, and A. J. Prata, "Atmospheric correction for satellite-based volcanic ash mapping and retrievals using split window IR data from GOES and AVHRR," *J. Geophys. Res.*, vol. 107, no. D16, p. 4311, Aug. 2002.

[10] S. Corradini, L. Merucci, and A. J. Prata, "Retrieval of SO_2 from thermal infrared satellite measurements: Correction procedures for the effects of volcanic ash," *Atmos. Meas. Tech.*, vol. 2, pp. 177–191, May 2009.

[11] R. S. J. Sparks, M. I. Bursik, S. N. Carey, J. S. Gilbert, L. S. Glaze, H. Sigurdsson, and A. W. Woods, *Volcanic Plumes*. Chichester, U.K.: Wiley, 1997.

[12] A. Folch, O. Jorba, and J. Viramonte, "Volcanic ash forecast—Application to the May 2008 Chaiten eruption," *Nat. Haz. Earth Syst. Sci.*, vol. 94, pp. 109–117, 2008.

[13] S. Scollo, A. Folch, M. Coltelli, and V. J. Realmuto, "3D volcanic aerosol dispersal: A comparison between MISR data and numerical simulations," *J. Geophys. Res.*, 2010, to be published.

[14] A. Costa, G. Macedonio, and A. Folch, "A three-dimensional Eulerian model for transport and deposition of volcanic ashes," *Earth Planet. Sci. Lett.*, vol. 241, no. 3/4, pp. 634–647, Jan. 2006.

[15] A. Folch, A. Costa, and G. Macedonio, "FALL3D: A computational model for transport and deposition of volcanic ash," *Comput. Geosci.*, vol. 35, no. 6, pp. 1334–1342, Jun. 2009.

[16] D. Andronico, S. Scollo, A. Cristaldi, and S. Caruso, "The 2002–03 Etna explosive activity: Tephra dispersal and features of the deposit," *J. Geophys. Res.*, vol. 180, pp. 123–134, 2008.

[17] P. Dellino, D. Mele, R. Bonasia, L. Braia, L. LaVolpe, and R. Sulpizio, "The analysis of the influence of pumice shape on its terminal velocity," *Geophys. Res. Lett.*, vol. 32, p. L21 306, Nov. 2003.

[18] J. Michalakes, J. Dudhia, D. Gill, T. Henderson, J. Klemp, W. Skamarock, and W. Wang, "The weather research and forecasting model: Software architecture and performance," in *Proc. 11th ECMWF Workshop Use High Performance Comput. Meteorol.,* W. Zwiefhofer and G. Mozdzynski, Eds., 2005.

[19] F. E. Volz, "Infrared optical constants of ammonium sulfate, Sahara dust, volcanic pumice and fly ash," *Appl. Opt.*, vol. 12, no. 3, pp. 564–568, Mar. 1973.

[20] C. A. Neal, R. G. McGimsey, C. A. Gardner, M. L. Harbin, C. J. Nye, and T. E. C. Keith, "Tephra-fall deposits from the 1992 eruptions of Crater Peak, Mount Spurr Volcano, Alaska: A preliminary report on distribution, stratigraphy, and composition," *U.S. Geol. Surv. Bull.*, vol. 2139, pp. 65–79, 1995.

[21] W. Rose and A. Durant, "Fine ash content of explosive eruptions," *J. Volcanol. Geotherm. Res.*, vol. 186, no. 1/2, pp. 32–39, Sep. 2009.

[22] S. A. Carn, L. L. Strow, S. de Souza-Machado, Y. Edmonds, and S. Hannon, "Quantifying tropospheric volcanic emissions with AIRS: The 2002 eruption of Mt. Etna (Italy)," *Geophys. Res. Lett.*, vol. 32, p. L02 301, Jan. 2005.